

SPECIAL PROJECT PROGRESS REPORT

All the following mandatory information needs to be provided. The length should *reflect the complexity and duration* of the project.

Reporting year 2024

Project Title: Investigating multi-decadal climate variations in seasonal forecasts: The role of aerosol and greenhouse gas forcings

Computer Project Account: spgbwrig

Principal Investigator: Mr. Matthew Wright
Dr. Antje Weisheimer (ECMWF; University of Oxford)
Prof. Tim Woollings (University of Oxford)

Affiliation: University of Oxford

Name of ECMWF scientist(s) collaborating to the project (if applicable) Dr. Antje Weisheimer (ECMWF and University of Oxford)
Dr. Tim Stockdale (ECMWF)

Start date of the project: January 2023

Expected end date: December 2025

Computer resources allocated/used for the current year and the previous one (if applicable)

Please answer for all project resources

		Previous year		Current year	
		Allocated	Used	Allocated	Used
High Performance Computing Facility	(units)	23,600,000	20,612,479	23,600,000	1,211,175
Data storage capacity	(Gbytes)	83,840	~20,000	189,130	~20,000

Summary of project objectives (10 lines max)

This project aims to build on the work of Weisheimer et al. (2017, 2022, 2023), to investigate multidecadal variations in seasonal hindcast skill throughout the twentieth century. The experiments run in this project will test hindcast skill's sensitivity to various sources of external forcing, initially focusing on aerosol loads and, later, greenhouse gas emissions.

We will work closely with the CONFESS project team at ECMWF to run hindcasts with perturbed aerosol mass mixing ratios. The hindcasts will be analysed, focusing on comparing the low skill mid-century period to the high-skill recent period, and quantifying the impact of aerosol forcing on seasonal forecast dynamic and thermodynamic responses.

Summary of problems encountered (10 lines max)

It took a few months to modify the IFS source code in such a way that we could run seasonal hindcasts initialised from ERA-20C, with time-varying aerosol forcings. This meant that the first set of simulations could not be run until the second half of 2023.

The CONFESS aerosol dataset that we are using only goes back to 1970. Therefore, we have had to modify and develop our own aerosol dataset (adapted from CMIP6 forcings), when we initially thought we may be able to use CONFESS's for years before 1970. This added a substantial amount of work and methodological development in the first year.

Analysing the results of the first set of experiments has led to an unexpected focus on the circulation off Africa, and mostly the impacts of natural aerosols – this is not a problem, as such, but a slight change of focus.

Summary of plans for the continuation of the project (10 lines max)

The analyses of the initial experiments (DJF runs in 1925-1950 and 1985-2010, with doubled, halved and 'best guess' aerosol mass mixing ratios) are ongoing: see preliminary results below, relating aerosol forcing changes to changes in weather and climate variables.

These results are informing the next set of experiments, which are likely to involve a combination of perturbing the aerosol mass mixing ratios in a more complex way (e.g., just the anthropogenic aerosols, and/or just changing aerosols over a specific region), running more start dates (e.g., JJA runs), and runs which will help us diagnose the role of ocean/atmosphere coupling.

We anticipate starting this next set of experiments by September. These experiments will enable us to make conclusions about how and why there are changes in tropical circulation due to aerosol forcing and quantify the impacts of aerosol forcing in different regions.

List of publications/reports from the project with complete references

N/A yet – we are still analysing results from the first set of experiments. Once these analyses are completed, it is possible that a publication will be submitted.

Summary of results

If submitted **during the first project year**, please summarise the results achieved during the period from the project start to June of the current year. A few paragraphs might be sufficient. If submitted **during the second project year**, this summary should be more detailed and cover the period from the project start. The length, at most 8 pages, should reflect the complexity of the project. Alternatively, it could be replaced by a short summary plus an existing scientific report on the project attached to this document. If submitted **during the third project year**, please summarise the results achieved during the period from July of the previous year to June of the current year. A few paragraphs might be sufficient.

In summary, so far this project has:

- Collaborated with ECMWF colleagues in the seasonal forecasting team, especially Tim Stockdale and Retish Senan, to develop an experimental set-up that enables time-varying aerosol concentrations to be used with Cy48r1 for initialisations from CERA-20C.
- Developed an aerosol dataset, based on the methodology employed by the CONFESS project, to adapt CMIP6 aerosol forcings for use in the modified IFS Cy48r1.
- Run a first set of experiments, initialised on 1 November every year in 1925-1950 and 1985-2010 for four months, with three aerosol forcings: a ‘best guess’, doubled mass mixing ratios, and halved mass mixing ratios.
- Started to analyse the results of these initial experiments (see below).
- Begun planning for the second phase of experiments, which will aim to improve our understanding of the impact of aerosol on seasonal forecasts and answer questions identified from the first set of experiments.

Our preliminary results show that:

- The aerosol dataset is consistent with other studies. The maximum impact on the radiation budget when the aerosols are doubled or halved is over central Africa and the tropical Atlantic Ocean, with impacts over India, China and southeast Asia in the 1985-2010 period.
- No significant impact on seasonal forecast skill is observed from doubling/halving aerosols in the IFS, for the large-scale climate indices analysed (Nino 3.4, IOD, PNA).
- The biggest impacts of increasing the aerosol loading are radiative, with significant changes in 2m temperature and sea-surface temperature in regions with large changes in aerosol forcing (net response to increased aerosol forcing is a cooling).
- The magnitude of the response to increased/decreased aerosol concentrations increases throughout the season, from December to February. This is the case for all variables analysed so far.
- There are significant local changes in circulation over west Africa and the tropical Atlantic Ocean when aerosols are doubled/halved. These changes are likely caused by Saharan desert dust, and aerosols associated with biomass burning in the Congo rainforest. When aerosol forcing is increased:
 - The aerosols cool the land, reducing 2m temperatures.
 - They also cool the sea, reducing SST in a pattern resembling an ‘Atlantic Nina’.
 - Since the land is cooled more than the sea, the land-sea temperature contrast is altered.
 - This causes the ITCZ to shift southwards, along with associated precipitation, outgoing longwave radiation, high- and low-level zonal winds, and cloud cover.

The next phase of experiments is still to be finalised, but will likely involve:

- Building on the current experiments to investigate the role of coupling, potentially by taking changes in ocean temperatures and heat content from the initial experiments and using these to adjust CERA-20C initial conditions for the next set of experiments. This will enable us to separate the impact of the aerosols on the ocean and atmosphere and investigate the role of coupling in the observed response.

- Running longer lead-time simulations e.g., up to 18 months, to investigate further the timescale of response to a sudden aerosol forcing change.
- Repeating experiments but initialising the forecasting model in May to give coverage of JJAS. This will enable us to study the South Asian and West African monsoons and their interactions with aerosols.
- Changing aerosol forcings in more sophisticated ways e.g., changing only the anthropogenic aerosols, and/or only the aerosols over specific regions.

See below for full details:

Aerosol forcing dataset development

The aerosol forcings used in this project were developed in collaboration with the CONFESS team working at ECMWF (see <https://confess-h2020.eu>). We were able to utilise some of the work the CONFESS project has undertaken to develop a time-varying aerosol scheme for the IFS. The model changes made by CONFESS enabled us to adapt Cy48r1 of the IFS to run time-varying aerosol forcing for initialisations from 1901 onwards, taking CERA-20C as initial conditions.

CONFESS have developed a time-varying aerosol dataset back to 1970 for the IFS, but not for earlier in the century. We used a similar methodology to produce a dataset with time-varying aerosols from 1850 to 2015, with aerosols updating in 5-year epochs, based on CMIP6 aerosol forcings, and tuned to the IFS. This involved taking aerosol forcings from the GFDL-ESM4 historical run CMIP6 experiments (Krasting et al., 2018). After this dataset had been re-gridded (coarsened) to match the required horizontal and vertical resolution for the IFS aerosol input data, we calculated the ratio between the 2015 mass mixing ratio and every epoch from 1850 to 2015, at every gridpoint and vertical level. This ratio was used to modify the CONFESS aerosol data, to give a 3D aerosol mass mixing ratio for all aerosol species in every epoch.

This method was applied to seven aerosol species which are active in the modified version of the IFS we are using. Five are time-varying: sulfates, black carbon (sub-divided into hydrophobic and hydrophilic), nitrate (sub-divided into fine and coarse), organic matter (sub-divided into hydrophobic and hydrophilic), and ammonium. Two are stationary in time, and sub-divided into three size-based bins: mineral dust and sea salt.

The ‘best guess’ aerosol column integrated mass mixing ratios (which are used directly for BestAer experiments and doubled (halved) for DoubAer (HalfAer) experiments) are shown in the appendix to this document, and the difference in the surface radiation budget between DoubAer and HalfAer are shown in Figure 1.

The impact of increasing aerosol forcing overall has the impact of reducing the net radiation at the surface over most of the globe. This is comprised of an increase in the longwave radiation reaching the surface, which is outweighed by a larger decrease in the shortwave radiation reaching the surface (not shown). Figure 1 shows that the largest differences in surface radiation budget between DoubAer and HalfAer are over central Africa and in the tropical Atlantic Ocean. There are also substantial differences over India, southeast Asia and China, particularly in 1985-2010.

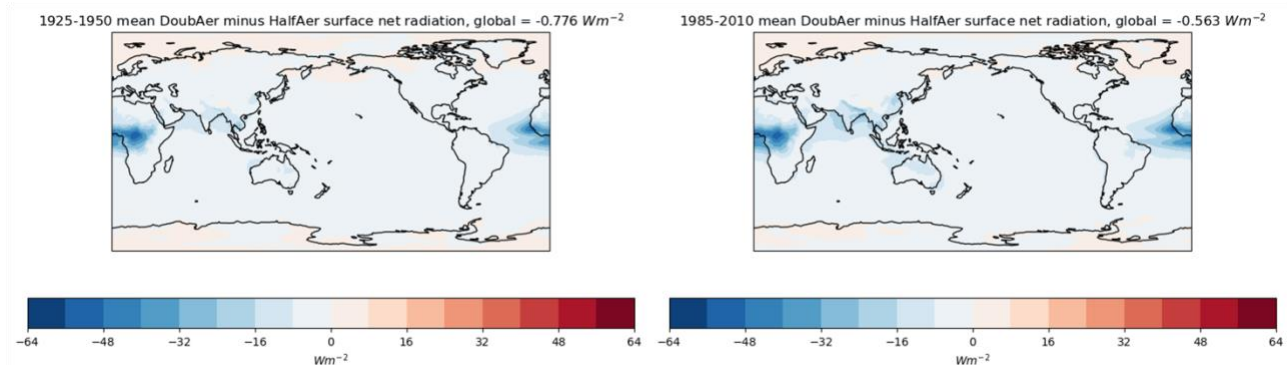


Figure 1: The DJF, ensemble mean difference in total (shortwave + longwave) radiation reaching the surface, between DoubAer experiments and HalfAer experiments. The values are averaged over the early period years (1925-1950, left), and the late period years (1985-2010, right). Negative values show regions where more radiation reaches the surface in HalfAer than DoubAer; vice-versa for positive values.

Experiments carried out in this special project

All experiments use a configuration of IFS Cycle 48r1 at resolution TCo199, with 91 vertical levels, coupled to the NEMO ocean model version 3.4, at 1° resolution, with 42 vertical levels. Initial conditions were from CERA-20C (Laloyaux et al., 2018) and all experiments had 21 ensemble members. Each experiment was initialised on November 1 in every year in 1925-1950 and 1985-2010, and run for four months. Each start date had three different aerosol forcings: one with ‘best guess’ aerosols described above, one with doubled aerosol forcing, and one with halved aerosol forcing. The experiments are summarised in Table 1.

Table 1: summary of model experiments performed so far.

Exp name	Early HalfAer	Early BestAer	Early DoubAer	Late HalfAer	Late BestAer	Late DoubAer
Years	1925-1950			1985-2010		
Aerosol mass mixing ratios	Half ‘best guess’	‘Best guess’	Double ‘best guess’	Half ‘best guess’	‘Best guess’	Double ‘best guess’

The experiments are compared to the ASF-20C and CSF-20C hindcast datasets, which are also initialised every November from 1901 to 2010 with fixed tropospheric aerosols. Full details can be found in Weisheimer et al. (2017, 2020).

Impact of changing aerosol forcing on seasonal hindcast skill

Our initial motivation for this special project was the multidecadal variability in seasonal hindcast skill identified in previous studies (e.g., Weisheimer (2017, 2020)). One hypothesis was that multidecadal variations in aerosol forcing influence seasonal hindcast skill. Our preliminary analysis indicates that this is not the case: Figure 2 shows that skill is almost independent – and certainly not correlated straightforwardly with – the level of aerosol forcing in the experiment. This is true for a range of large-scale climate indices, including Nino 3.4 (Figure 2a) and the Pacific-North American (PNA) teleconnection pattern (Figure 2b).

The Nino 3.4 index skill is invariant under different aerosol forcings, with skill consistent between CSF-20C (with fixed aerosol forcing) and all three aerosol experiments. This is, perhaps, expected, as a large component of skill in ENSO comes from the initial conditions. The PNA shows some variation in skill between the three recent experiments and the ASF-20C and CSF-20C hindcasts. However, this is not in a systematic way, and differences between experiments are much smaller than the ensemble spread within individual experiments.

We conclude that, for the seasonal-mean large-scale climate indices we have investigated, there is no significant relationship between seasonal hindcast skill and the aerosol forcing.

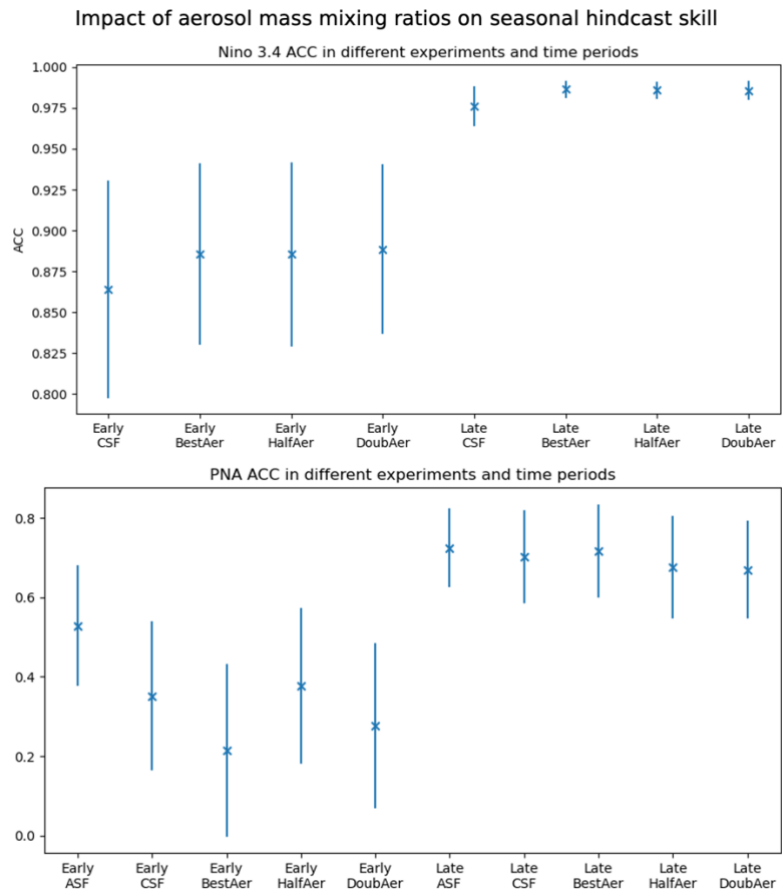


Figure 2: Anomaly correlation coefficient (see <https://confluence.ecmwf.int/display/FUG/Section+6.2.2+Anomaly+Correlation+Coefficient>) calculated for CSF-20C, ASF-20C (PNA only), and all three new experiments, for the periods 1925-1950 ('early') and 1985-2010 ('late'). BestAer is forced by 'best guess' aerosols calculated from CMIP6 forcings and adjusted for use in the IFS; DoubAer doubles the mass mixing ratios of BestAer; HalfAer halves the mass mixing ratios of BestAer. The error bars show the ensemble standard deviation in the skill of the index.

Impact of changing aerosol forcing on spatial-temporal weather and climate variables

We have investigated the impact of changing the aerosol forcings on various weather and climate variables, in both the early (1925-1950) and late (1985-2010) periods. For all variables, the response is similar in both the early and late periods, so the results in the rest of this report focus on the average differences across all years (1925-1950 and 1985-2010). This can be thought of as a way to test the model's response to changed aerosol forcing, whilst sampling a range of different initial conditions from across the 20th century.

Figure 3 shows the difference between the doubled aerosol experiment and halved aerosol experiment for 2m temperature and sea-surface temperatures (SSTs) i.e., the global response to a quadrupling of aerosol mass mixing ratios from half of 'best guess' to double 'best guess'. There is clearly a response local to large changes in aerosol mass mixing ratio i.e., areas with large aerosol forcings to start with. We interpret this as a radiative response due to the increased (decreased) radiation reaching the surface in the halved (doubled) experiments compared to the 'best guess' experiment.

The most notable features in Figure 3 are the large cooling response to increased aerosol concentration over central and western Africa, which is matched by a cooling response in the SSTs

in the eastern tropical Atlantic Ocean, off the west African coast. This resembles an Atlantic Nina pattern (Zebiak, 1993). There are further regions of significant cooling responses over northern India, the Tibetan Plateau, eastern China, and the interior of Australia. The radiative responses over Africa, Tibet and Australia are likely driven by mineral dust concentrations, and those over India and China by sulfate and black carbon.

Furthermore, the magnitude of the response of 2m temperatures and SSTs increases throughout the season, from December to February (not shown). This is true for all other variables investigated as well. This shows that the model is still adjusting to the effective step-change in aerosol at the initialisation date, and that the effect of the aerosols on the weather and climate is continuing to grow. It would be useful to have longer integrations (see Next Steps) in order to find the timescale for the response to stabilise.

Response of DJF-mean surface temperature and sea surface temperature to increased aerosol forcing

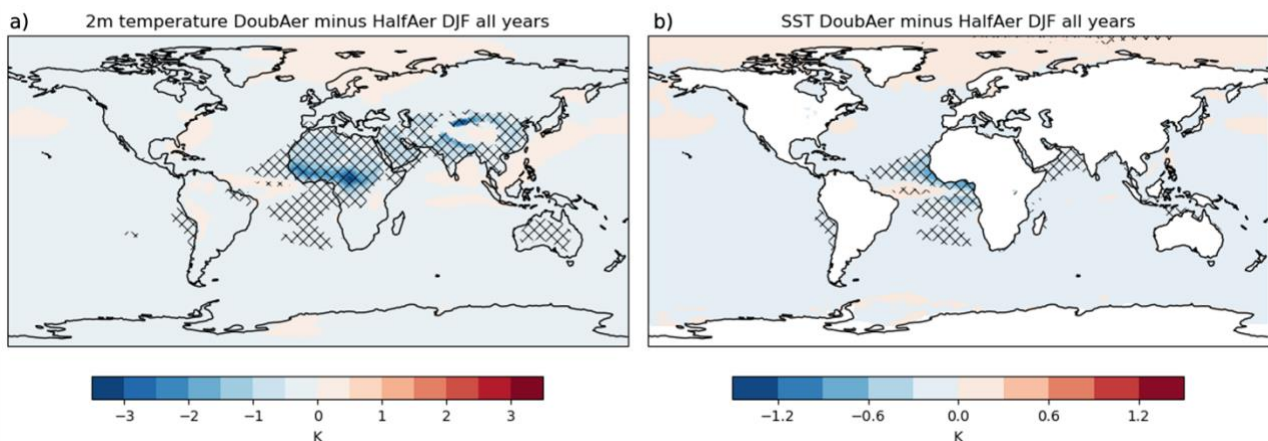


Figure 3: The DJF, ensemble mean difference in (a) 2m temperature, and (b) sea-surface temperature (SST), between DoubAer experiments and HalfAer experiments. The values are averaged over all years in both periods (1925-1950 and 1985-2010). Negative values show regions where the temperature is cooler in DoubAer than HalfAer; vice-versa for positive values. Hatching indicates significance at the 5% level, using a student's *t*-test.

As the largest changes in surface radiation budget, 2m temperature and SST are seen over western Africa and the tropical Atlantic Ocean, we have analysed the differences between the experiments in this region in greater detail.

Figure 4 shows the differences between DoubAer and HalfAer experiments in a range of climate variables. There is a clear shift of precipitation southwards (a) which, along with changes in outgoing longwave radiation (b) and total cloud cover (c), indicate that the inter-tropical convergence zone (ITCZ) has migrated southwards (Schneider et al., 2014) when aerosol forcing was increased. This was confirmed by analysing the latitude of the moist static energy maximum (not shown), which gives the position of the thermal equator. The moist static energy maximum shift indicates a local southward shift of the ITCZ over the eastern tropical Atlantic Ocean, with no significant changes over land. The high-level (e) and low-level (f) winds show that there is a weakening of the Walker cell over the southern Tropical Atlantic Ocean (Wang, 2004).

We attribute these changes to an altered land-sea contrast in DoubAer compared to HalfAer. In DoubAer, the land over west Africa is cooled relative to the sea (although both the land and sea are cooler than in BestAer/HalfAer). This can be seen in Figure 3a, where the land 2m temperatures cool more strongly than those over the ocean. This causes a positive pressure anomaly to develop over land, and a low-pressure anomaly over the ocean. This reduces the magnitude of winds blowing from the ocean to the land, reducing the amount of moisture and thus reducing precipitation. This is a similar mechanism to the summer monsoon circulation over west Africa (Sultan and Janicot, 2003), but with the opposite sign. In the case of the aerosol experiments,

because the land north of the equator cools more than the land south of the equator, and the ITCZ shifts southwards.

Increased aerosol forcing's impact on seasonal mean weather variables over the tropical Atlantic Ocean and west Africa

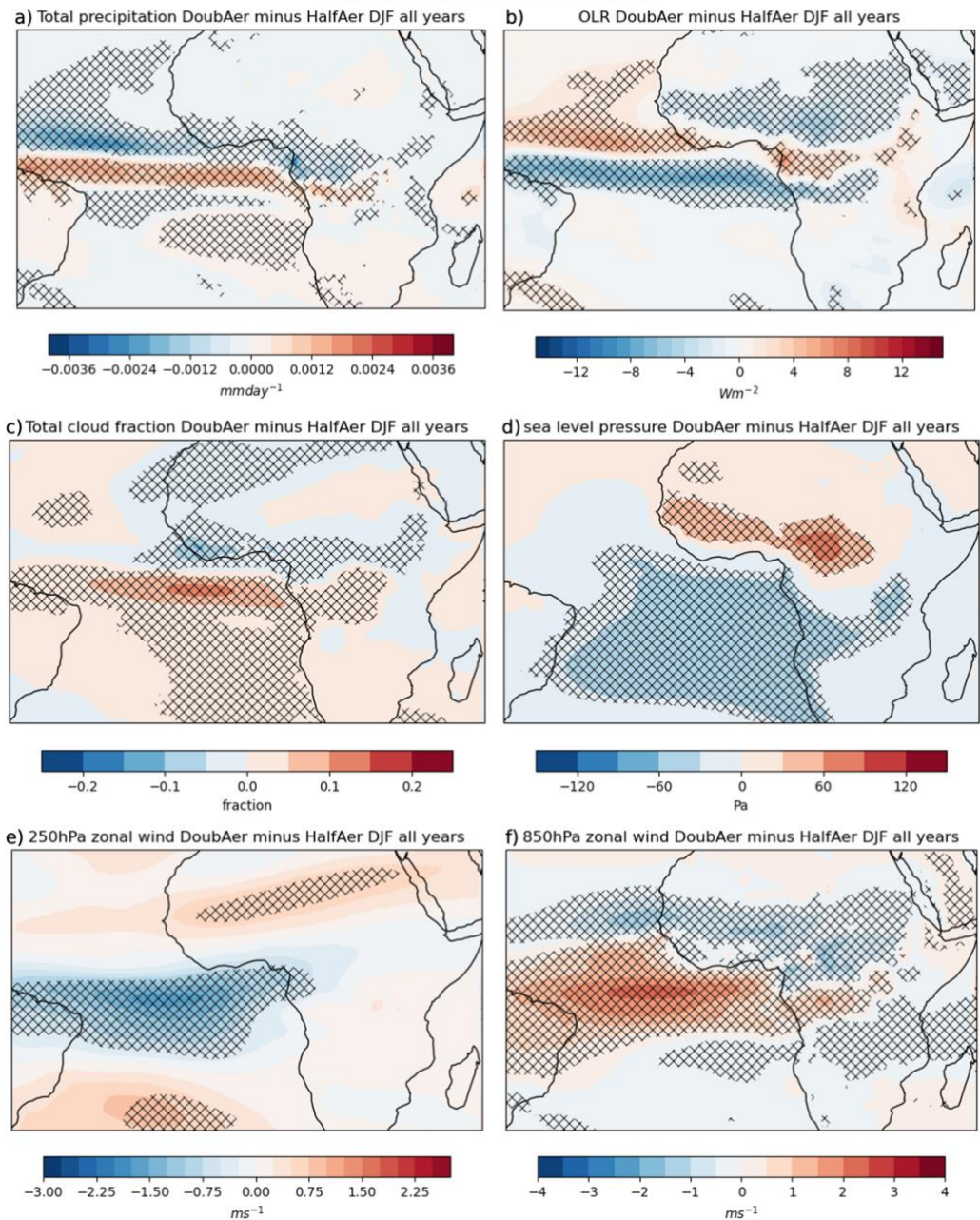


Figure 4: The DJF, ensemble mean difference in (a) precipitation rate, (b) outgoing longwave radiation (OLR), (c) total cloud fraction, (d) sea level pressure, (e) 250hPa zonal wind, and (f) 850hPa zonal wind, between DouBAer experiments and HalfAer experiments, over Africa and the tropical Atlantic Ocean. The values are averaged over all years in both periods (1925-1950 and 1985-2010). Negative values show regions where the value is lower in DouBAer than HalfAer; vice-versa for positive values. Hatching indicates significance at the 5% level, using a student's t-test.

These results show the importance of Congo biomass burning and Saharan desert dust on the position of the ITCZ and precipitation across the eastern tropical Atlantic and west Africa. There is the potential for these aerosol sources to increase in a future, warming, climate. This mechanism, therefore, warrants further investigation.

Further analyses and next steps

Further analyses are being conducted to complete the story presented above, and we hope to write this up into a publication in the near future.

The next set of experiments will build on these results to explore the role of coupling, with possibilities including:

- Initialising hindcasts in May, to capture the west African and South Asian monsoon season JJAS, to compare the impact on the monsoon circulation with the mechanism identified above in DJF.
- Running longer hindcasts (up to 18 months long), to investigate further the timescale of the oceanic and atmospheric response to the step-change in aerosol forcing.
- Using the SST differences between BestAer and DoubAer (HalfAer) to re-run DoubAer (HalfAer) experiments with adjusted initial conditions (current initial conditions + SST difference), which will help us diagnose the role of coupling on the response to aerosol forcing.
- Perturbing anthropogenic aerosols only, and/or only aerosols in specific regions of the world.

These experiments are in development and will be prioritised based on discussions within the project team, with our collaborators at ECMWF, and other academics working in this area.

References

Krasting, John P.; John, Jasmin G; Blanton, Chris; McHugh, Colleen; Nikonov, Serguei; Radhakrishnan, Aparna; Rand, Kristopher; Zadeh, Niki T.; Balaji, V; Durachta, Jeff; Dupuis, Christopher; Menzel, Raymond; Robinson, Thomas; Underwood, Seth; Vahlenkamp, Hans; Dunne, Krista A.; Gauthier, Paul PG; Ginoux, Paul; Griffies, Stephen M.; Hallberg, Robert; Harrison, Matthew; Hurlin, William; Malyshev, Sergey; Naik, Vaishali; Paulot, Fabien; Paynter, David J; Ploshay, Jeffrey; Reichl, Brandon G; Schwarzkopf, Daniel M; Seman, Charles J; Silvers, Levi; Wyman, Bruce; Zeng, Yujin; Adcroft, Alistair; Dunne, John P.; Dussin, Raphael; Guo, Huan; He, Jian; Held, Isaac M; Horowitz, Larry W.; Lin, Pu; Milly, P.C.D; Shevliakova, Elena; Stock, Charles; Winton, Michael; Wittenberg, Andrew T.; Xie, Yuanyu; Zhao, Ming (2018). *NOAA-GFDL GFDL-ESM4 model output prepared for CMIP6 CMIP historical*. Version 20230501. Earth System Grid Federation. <https://doi.org/10.22033/ESGF/CMIP6.8597>

Laloyaux, P., de Boisseson, E., Balmaseda, M., Bidlot, J.-R., Broennimann, S., Buizza, R., et al. (2018). *CERA-20C: A coupled reanalysis of the twentieth century*. Journal of Advances in Modeling Earth Systems, 10, 1172–1195. <https://doi.org/10.1029/2018MS001273>

Schneider, T., Bischoff, T. & Haug, G (2014). *Migrations and dynamics of the intertropical convergence zone*. Nature 513, 45–53. <https://doi.org/10.1038/nature13636>

Sultan, B., and S. Janicot (2003). *The West African Monsoon Dynamics. Part II: The “Preonset” and “Onset” of the Summer Monsoon*. J. Climate, 16, 3407–3427, [https://doi.org/10.1175/1520-0442\(2003\)016<3407:TWAMDP>2.0.CO;2](https://doi.org/10.1175/1520-0442(2003)016<3407:TWAMDP>2.0.CO;2)

Wang, C. (2004). *ENSO, Atlantic Climate Variability, and the Walker and Hadley Circulations*. In: Diaz, H.F., Bradley, R.S. (eds) *The Hadley Circulation: Present, Past and Future*. Advances in Global Change Research, vol 21. Springer, Dordrecht. https://doi.org/10.1007/978-1-4020-2944-8_7

Weisheimer, A., Schaller, N., O'Reilly, C., MacLeod, D.A. and Palmer, T. (2017), *Atmospheric seasonal forecasts of the twentieth century: multi-decadal variability in predictive skill of the winter North Atlantic Oscillation (NAO) and their potential value for extreme event attribution*. Q.J.R. Meteorol. Soc, 143: 917-926. <https://doi.org/10.1002/qj.2976>

Weisheimer, A., D. J. Bafort, D. MacLeod, T. Palmer, C. O'Reilly, and K. Strømme (2020). *Seasonal Forecasts of the Twentieth Century*. Bull. Amer. Meteor. Soc., 101, E1413–E1426, <https://doi.org/10.1175/BAMS-D-19-0019.1>

Zebiak, S. E. (1993). *Air–Sea Interaction in the Equatorial Atlantic Region*. J. Climate, 6, 1567–1586, [https://doi.org/10.1175/1520-0442\(1993\)006<1567:AIITEA>2.0.CO;2](https://doi.org/10.1175/1520-0442(1993)006<1567:AIITEA>2.0.CO;2)

Appendix

BestAer average mass mixing ratios, 1925-1950

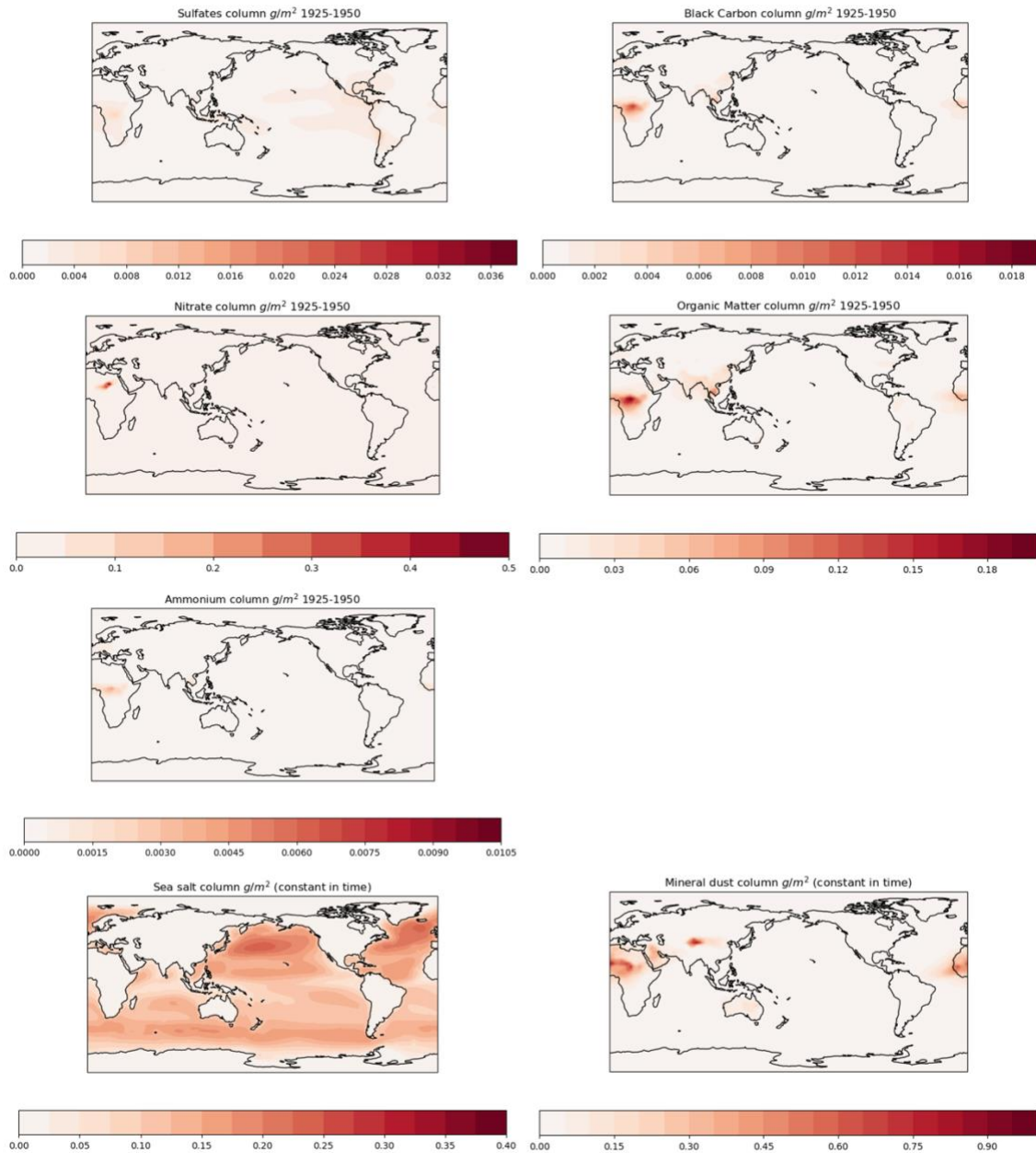


Figure 5: Vertically integrated aerosol concentrations for the aerosol 'best guess' dataset developed during this project, shown for all species which are active in the IFS version we are using for this project. The values shown are summed over all vertical levels to give a column mass in grams per square metre. Where a species is divided into bins or types, these are added together to produce a total column for that species. This is then averaged over the period 1925-1950 (except for mineral dust and sea salt, which are stationary in time) to produce the maps shown. Note the different colourbar for each plot.

BestAer average mass mixing ratios, 1985-2010

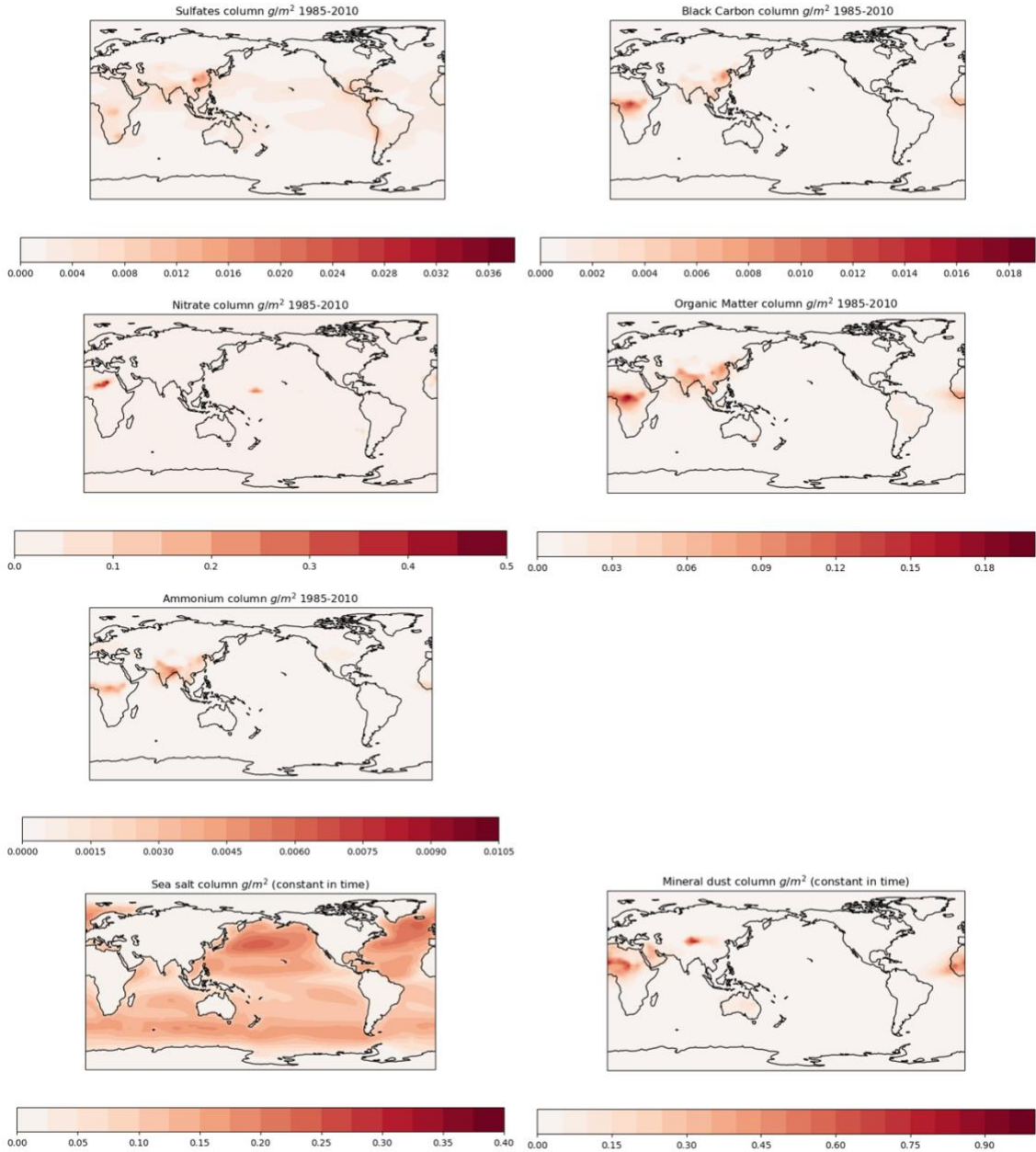


Figure 6: Vertically integrated aerosol concentrations for the aerosol 'best guess' dataset developed during this project, shown for all species which are active in the IFS version we are using for this project. The values shown are summed over all vertical levels to give a column mass in grams per square metre. Where a species is divided into bins or types, these are added together to produce a total column for that species. This is then averaged over the period 1925-1950 (except for mineral dust and sea salt, which are stationary in time) to produce the maps shown. Note the different colourbar for each plot.